Nörogörüntülemenin vaadleri, katkıları, teknik açmazlar ve fırsatlar

Didem Gökçay

didemgokcay@gmail.com

Nörogörüntülemenin vaadleri

Beynin yapısının mikro ve makro düzeyde görüntülenmesi

https://www.youtube.com/watch?v=dxl5DOnd-MA

Ed Boynton Lab and Nova Inc movie

Beynin yapısının mikro ve makro düzeyde görüntülenmesi

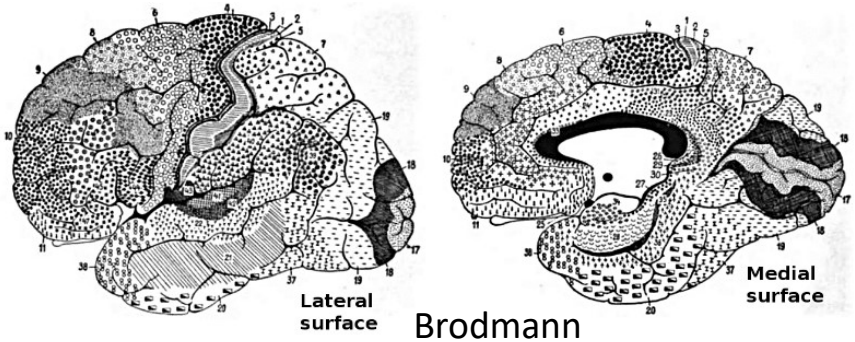

Brodmann

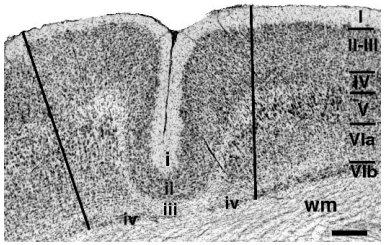

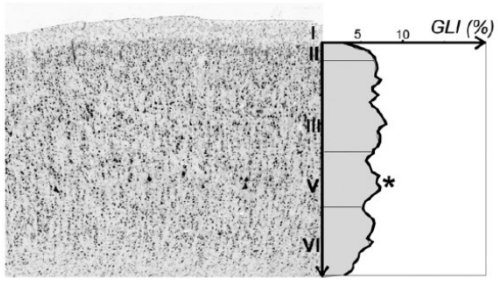

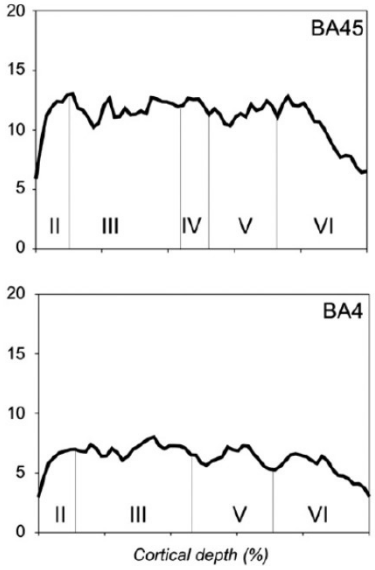

Amunts, 2007

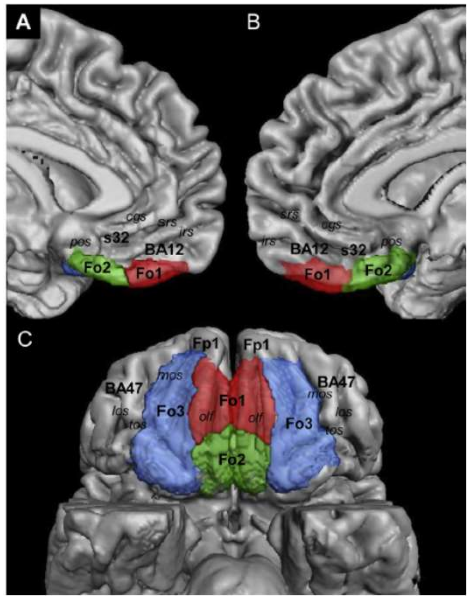

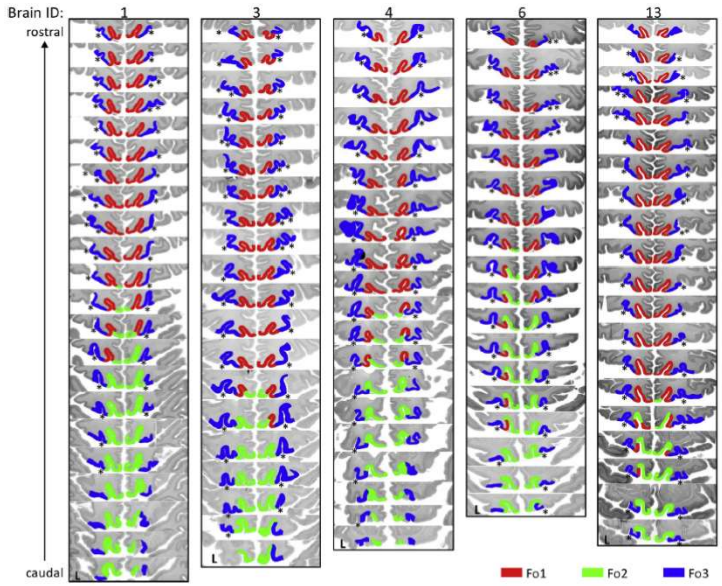

Amunts, 2016

Beynin işlevinin mikro ve makro düzeyde görüntülenmesi

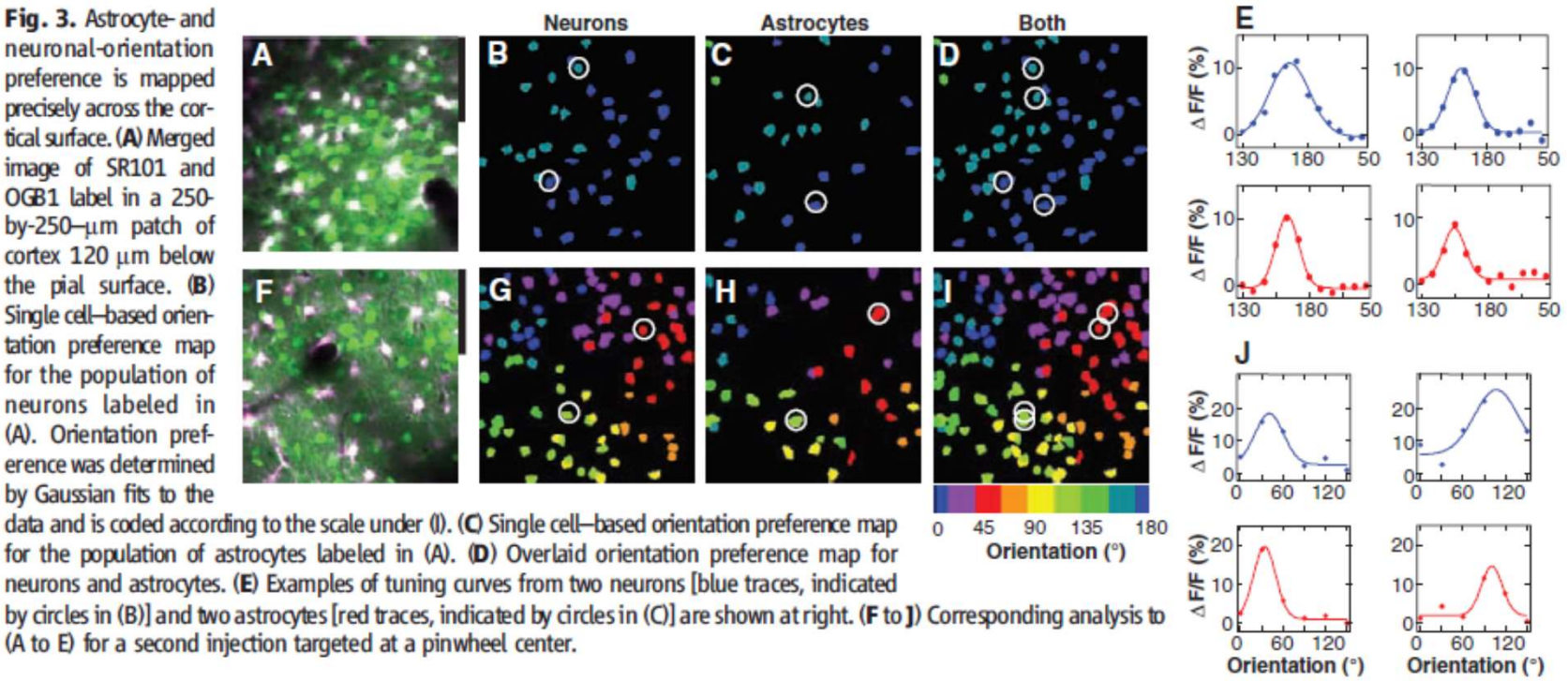

Fig. 3. Astrocyte- and neuronal-orientation preference is mapped precisely across the cortical surface. (**A**) Merged image of SR101 and OGB1 label in a 250-by-250–μm patch of cortex 120 μm below the pial surface. (**B**) Single cell–based orientation preference map for the population of neurons labeled in (A). Orientation preference was determined by Gaussian fits to the data and is coded according to the scale under (I). (**C**) Single cell–based orientation preference map for the population of astrocytes labeled in (A). (**D**) Overlaid orientation preference map for neurons and astrocytes. (**E**) Examples of tuning curves from two neurons [blue traces, indicated by circles in (B)] and two astrocytes [red traces, indicated by circles in (C)] are shown at right. (**F** to **J**) Corresponding analysis to (A to E) for a second injection targeted at a pinwheel center.

Schummers, 2008

Beynin işlevinin mikro ve makro düzeyde görüntülenmesi

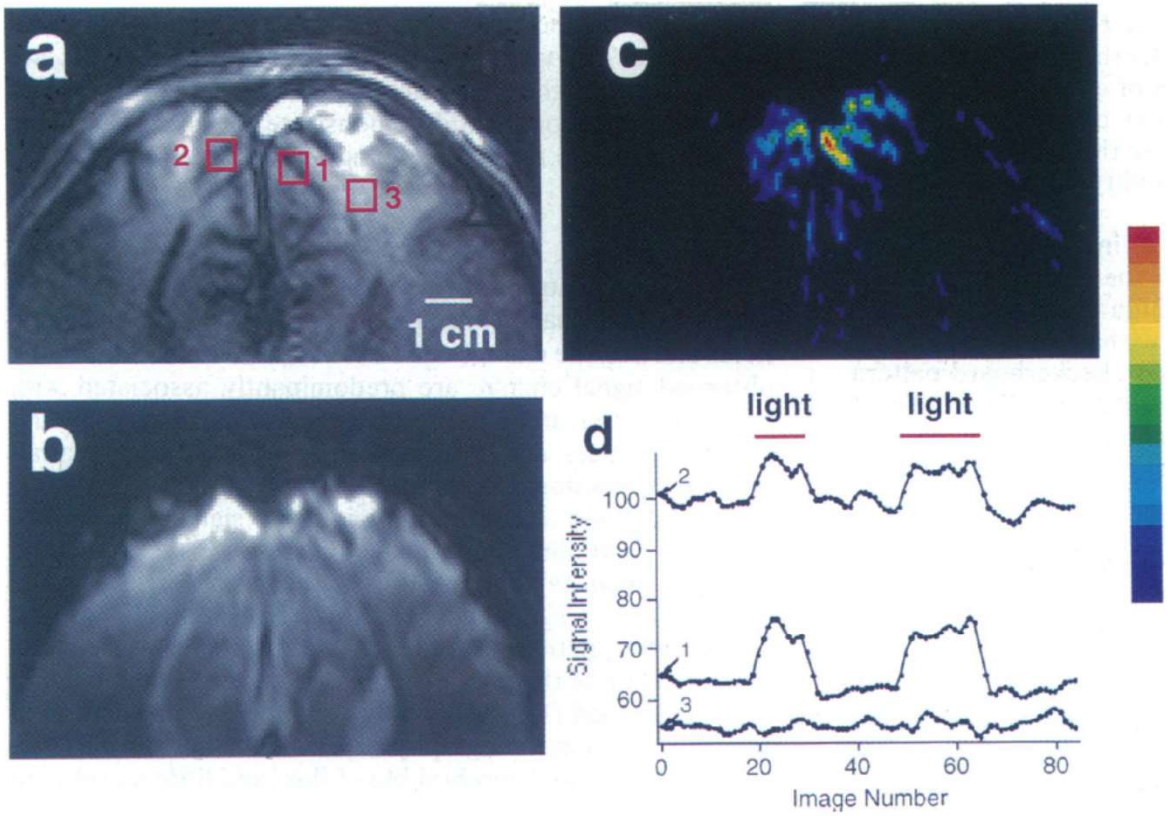

Ogawa et al, 1992

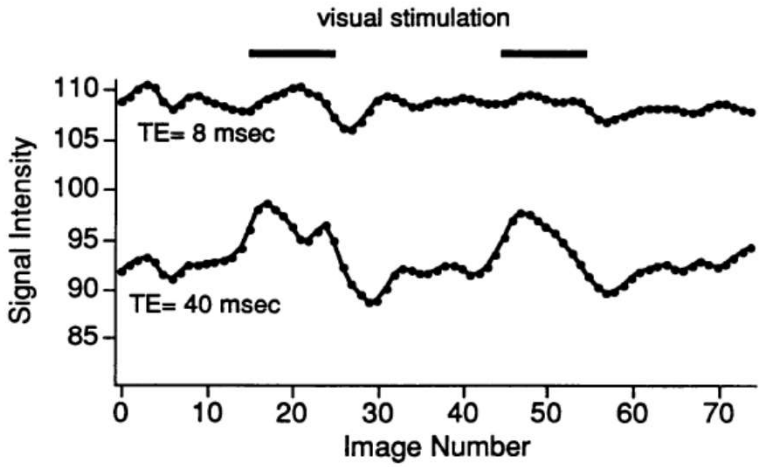

FIG. 3. Reducing TE reduces amplitude of the visual stimulation-induced intrinsic signal change. The time course of intrinsic signal changes observed at a fixed caudal position in primary visual cortex are shown for TE = 40 ms and TE = 8 ms. Other experimental conditions were as in Fig. 2, except that patterned-flash visual stimulation was provided between images 15–25 and 35–55.

Beynin işlevinin mikro ve makro düzeyde görüntülenmesi

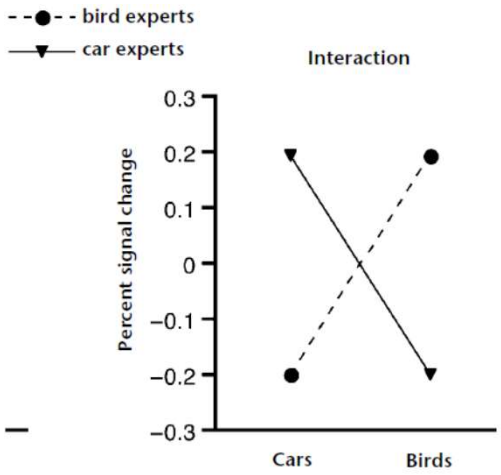

11 car experts
8 bird experts

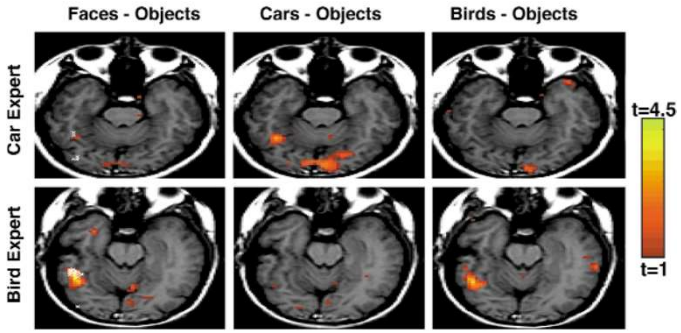

Gauthier 2000

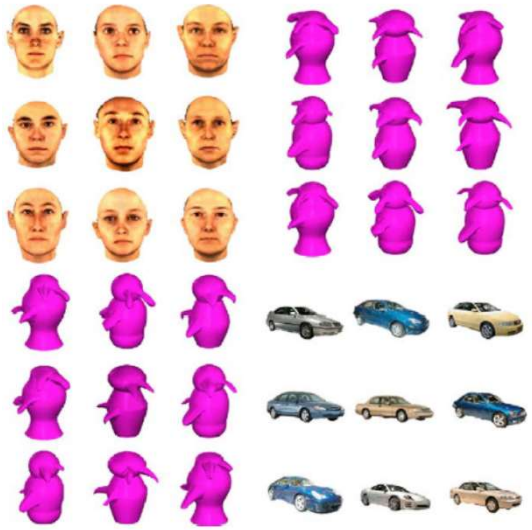

Birden fazla düzeydeki bulguların entegrasyonu

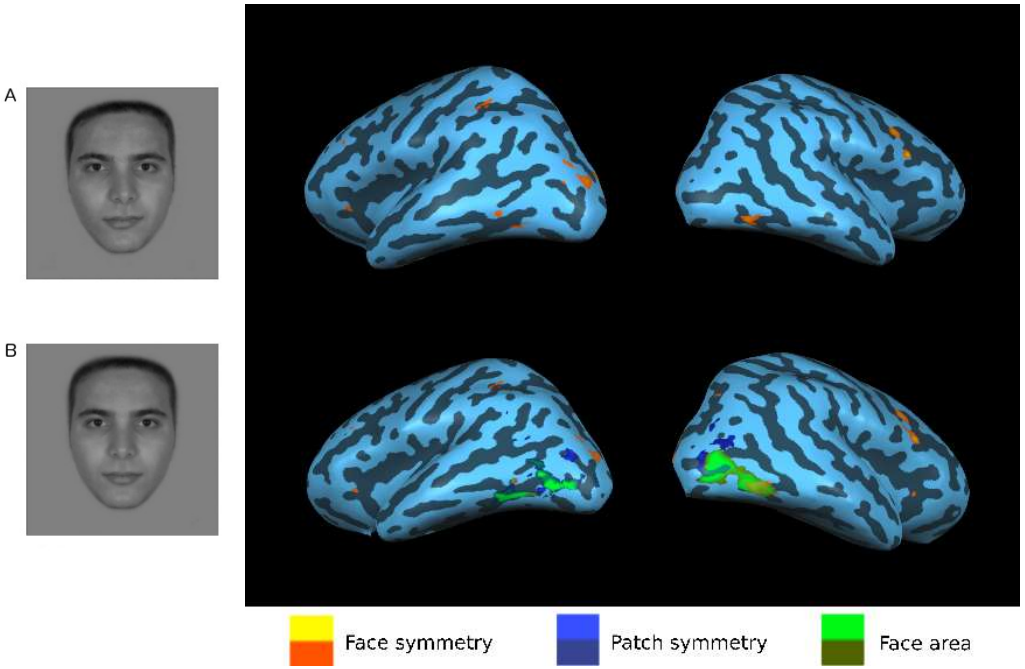

Gokcay, Yıldırım, Yıldırım, Hepsomalı, 2014

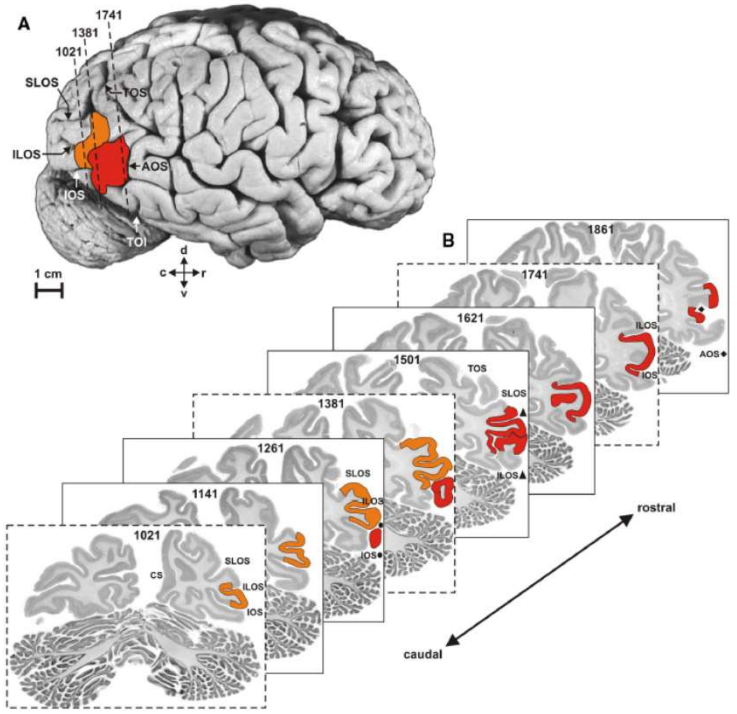

Fig. 4 Location and extent of areas hOc4la (*red*) and hOc4lp (*orange*) on the surface of brain number 10 (**a**) and in a selection of histological serial sections (**b**). The *dashed lines* in panel **a** show the approximate level of Section *1021*, *1381* and *1741* in panel B. *AOS* anterior occipital sulcus, *CS* calcarine sulcus, *ILOS* inferior lateral occipital sulcus, *IOS* inferior occipital sulcus, *SLOS* superior lateral occipital sulcus, *TOI* temporo-occipital incisure, *TOS* transverse occipital sulcus. *Cross arrow*: *c* caudal, *d* dorsal, *r* rostral, *v* ventral

Katrin Amunts, 2016

Beynin haritalan**ma**mış kısımlarına yönelik araştırmalar

Erken evre görsel korteksin hacmi

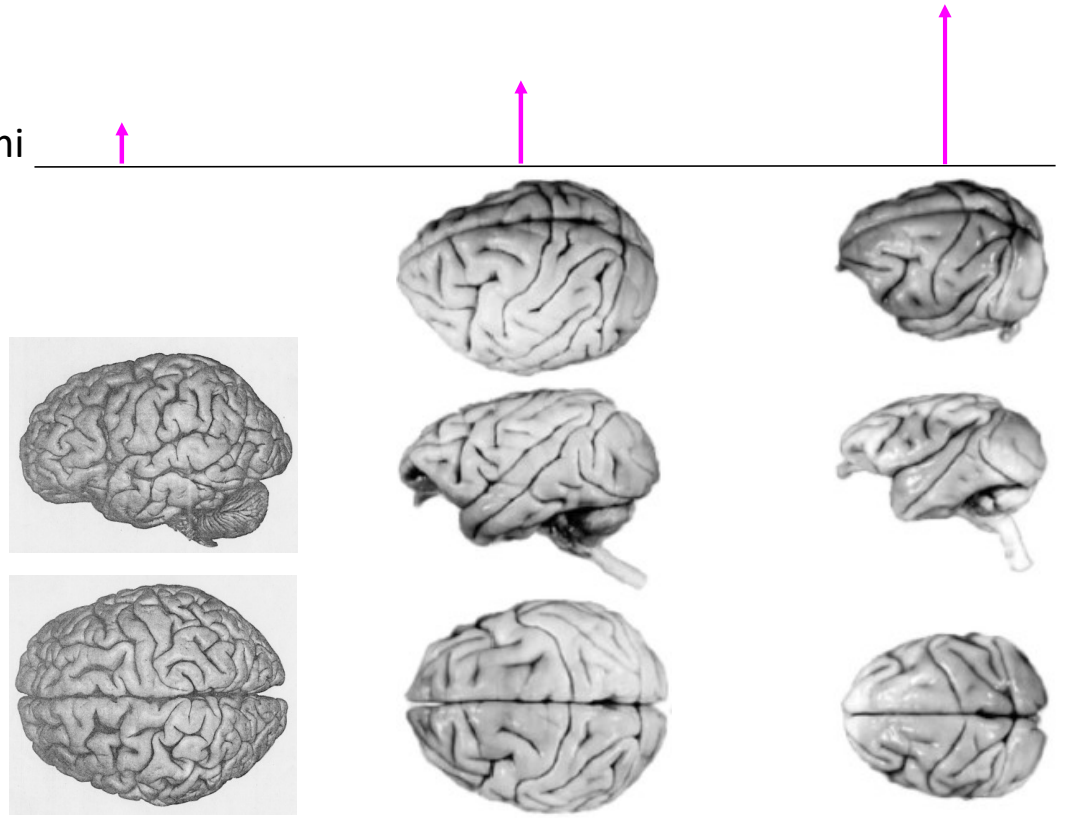

Human

Hamadryas Baboon
large bodied

Rhesus monkey
small bodied

Primatlarda vücut ve beyin büyüdükçe,
primer görsel korteksin beyne oranı küçülmektedir.
(Insan, şempanze ve makakta bu oranlar 3, 6, 12 % dir)
Yani haritalanmamış kısım insanda en büyüktür...

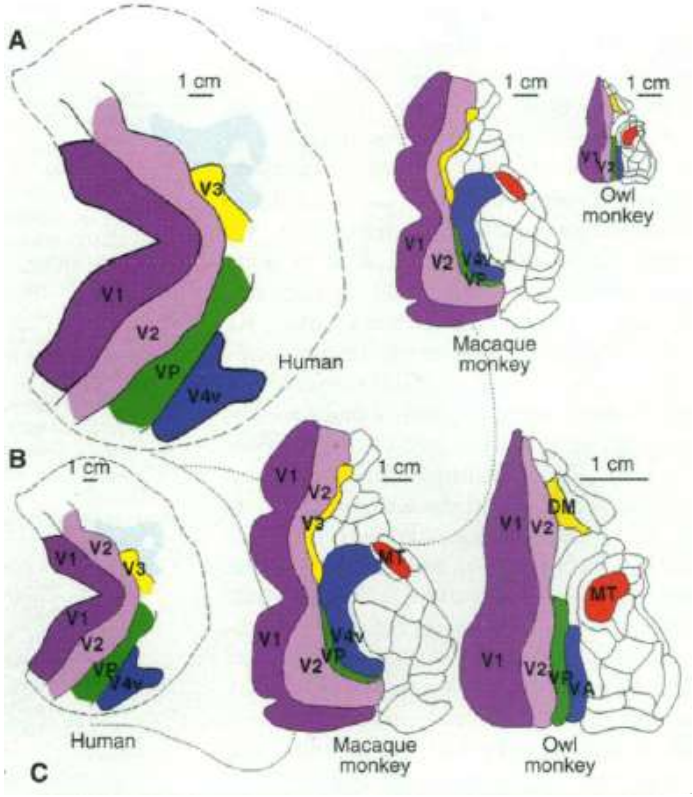

Sereno, 1995

EMO BMO SUNUM 2019

Yeni haritalama teknikleri

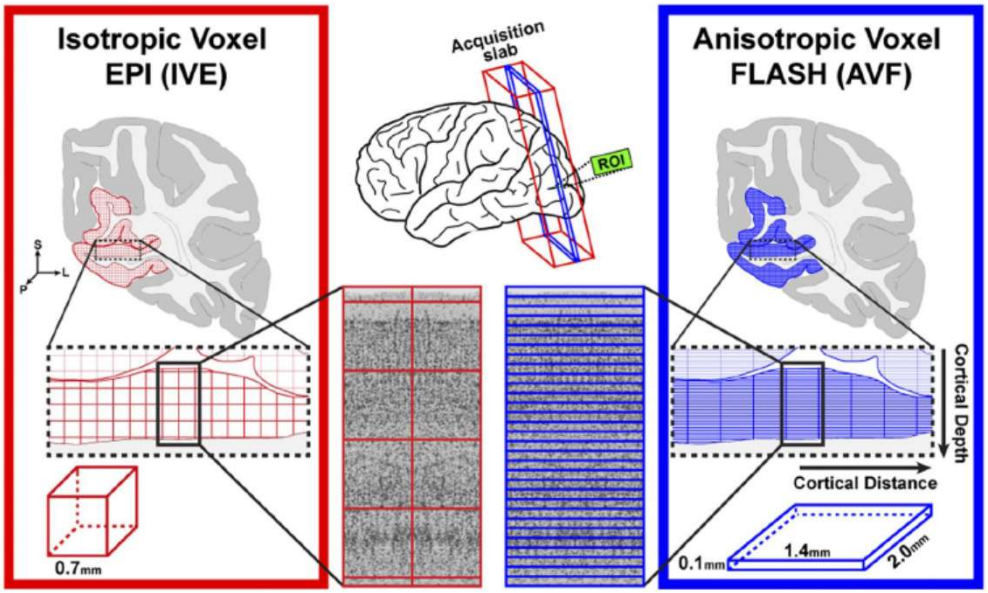

Figure 1. Illustration of the IVE (left, red) and the novel AVF (right, blue) acquisition schemes for layer-specific fMRI, highlighting the differences in the sampling of cortical depths between the two approaches.

Laminar fMRI,
John Polimeni

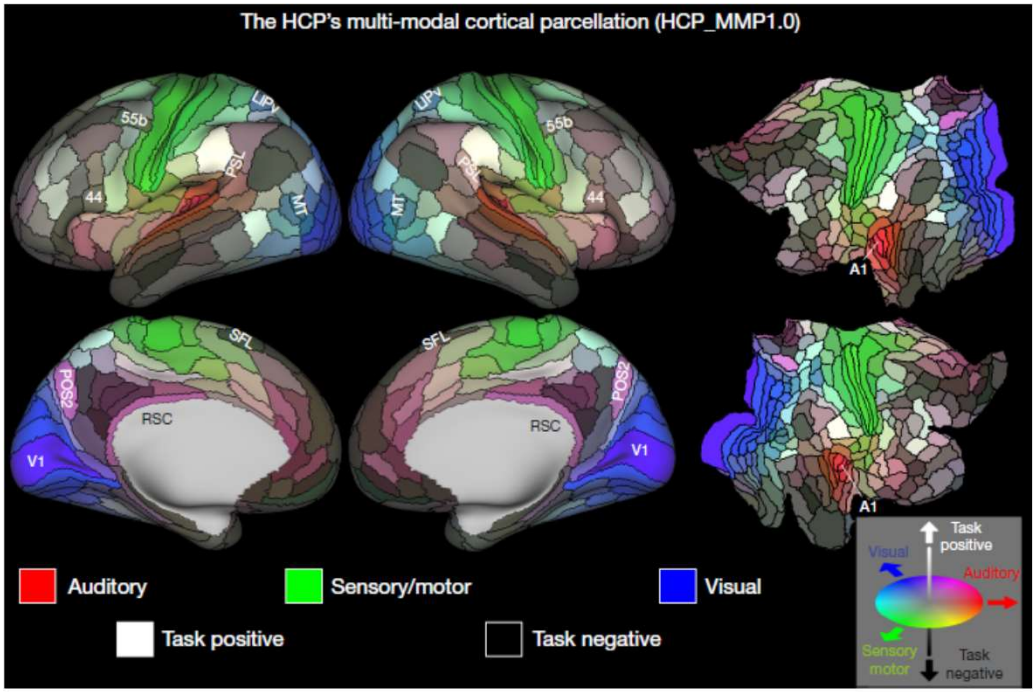

Multi-modal parcellation (BRAIN Initiative)
Kamil Uğurbil, et al. 2016

Tanı ve tedaviye yönelik uygulamalar

İkili sınıflandırma: Klinik hastalıklarda sınıflandırma uygulamaları

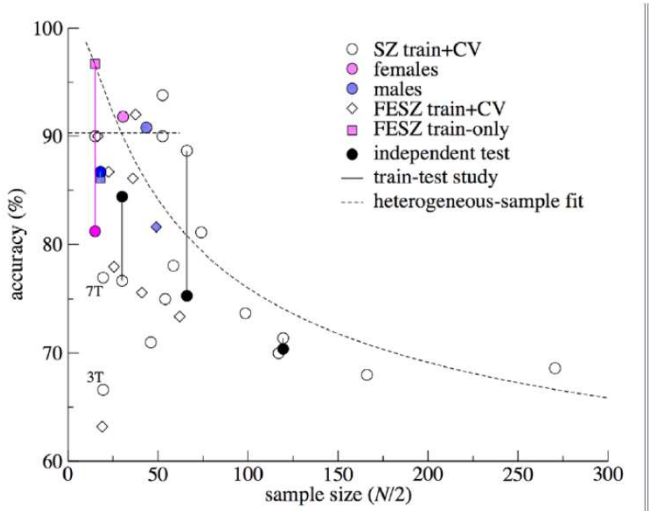

FIGURE 1 | Prediction accuracy versus sample size for the schizophrenia machine learning studies using structural MRI. Data are taken from the reviews by Zarogianni et al. (9) and Kambeitz et al. (1) and some (recent) studies (4, 14–18). Sample size *N*/2 was calculated as the mean of the patient and control sample sizes. Different symbols mark cross-validation accuracy from studies on chronic/mixed patients (circles) and first-episode patients (diamonds). Soft colors were used to indicate studies that included only females (pink) or males (blue). Train accuracy without cross-validation is marked by squares. Lines connect train–test studies, where the accuracy in the independent test sample is marked with solidly filled symbols. "3T" and "7T" mark the study by Iwabuchi (19), using the same subjects scanned at different field strengths. Curved dashed line: heterogeneous-sample theory. Horizontal dashed line: stretched range of homogeneous samples.

Schnack & Kahn 2016

Nörogörüntülemenin katkıları

Beyinciğin bilişsel ve duygusal işlevleri

a single-subject level, we conducted functional magnetic resonance imaging (fMRI) during five tasks investigating sensorimotor (finger tapping), language (verb generation), spatial (mental rotation), working memory (N-back), and emotional processing (viewing images from the International Affective Picture System). Finger tapping activated the ipsilateral anterior lobe (lobules

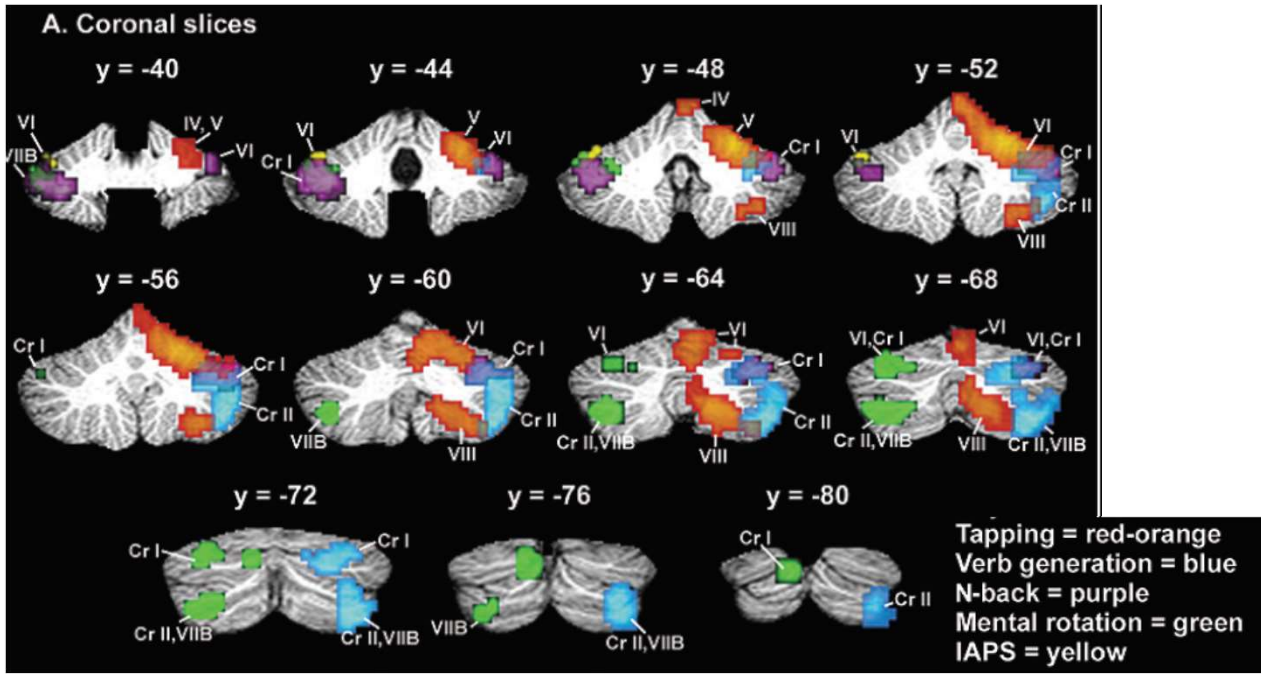

Schmahmann, 2010

Duyguların primitif algılar ile etkileşimi

Postravmatik stres hastalığında, duygusal algılara karşı subliminal düzeyde dahi hassasiyet gözlenir

Deney:

20 Israelli asker, 10 tanesi PTS hastası

Uyaran: 280 resim
Yarısı savaş içerikli

Resimler 20, 40, 80 msn boyunca gösterilmiş
500 msn süreli maske uygulanmış

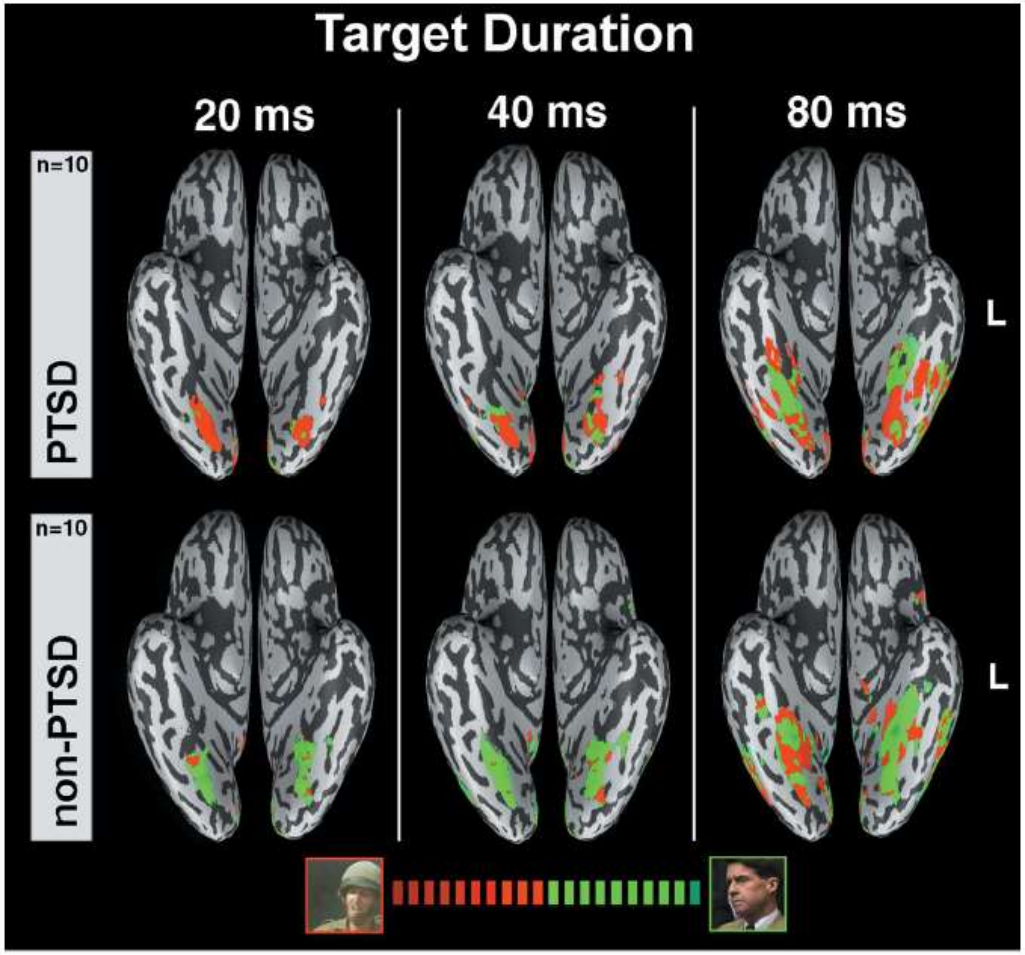

Fig. 2. Content effect per group in LOC. Parametric activation maps for PTSD (n = 10, upper row) and non-PTSD (n = 10, bottom row) subjects. Each map was obtained by using multistudy GLM (uncorrected fixed threshold, $P < 0.002$) with combat and noncombat contents as predictors represented by two colors, and shown separately for each target duration (20, 40, and 80 ms). Activated clusters are shown from a ventral view on one inflated brain. Red clusters stand for stronger relative contribution for the combat stimuli, and green clusters represent stronger relative contribution for the noncombat stimuli. L, left; ms, milliseconds.

Hendler, 2003

Beynin dinlenme durumundaki faaliyetleri

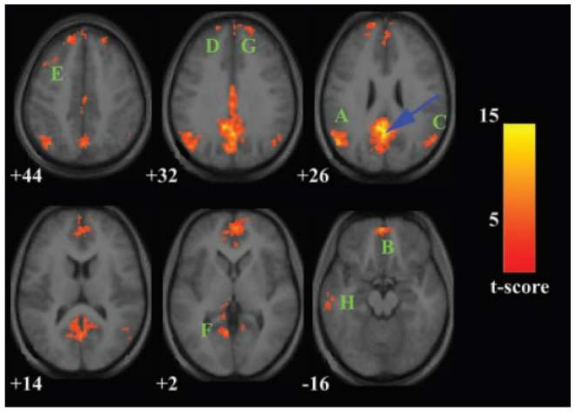

Fig. 1. Map of the resting-state neural connectivity for the PCC. The blue

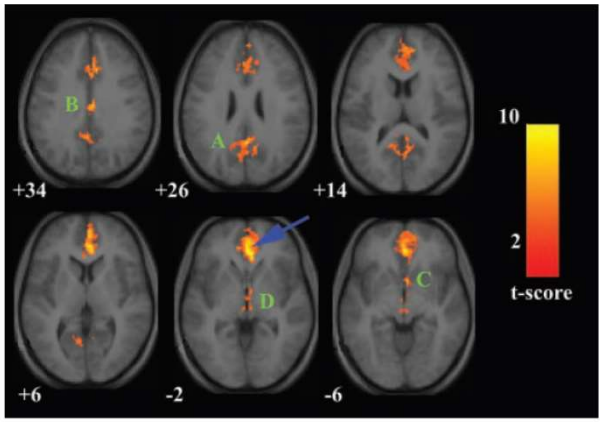

Fig. 2. Map of the resting-state neural connectivity for the vACC. The blue

Greicius 2003

Connected regions	BA
PCC/precuneus	23/31/7
Left IPC	39/40
OFC/MPFC/vACC	11/10/32
Right IPC	39/40
MPFC	8
Left DLPFC	8/9
Left PHG	30
MPFC	9
Left ITC	20/21

Connected regions	BA
VACC/MPFC/OFC	32/10/11
PCC/precuneus	23/31/7
Rostral PCC	23
Nucleus accumbens	N/A
Hypothalamus/midbrain	N/A

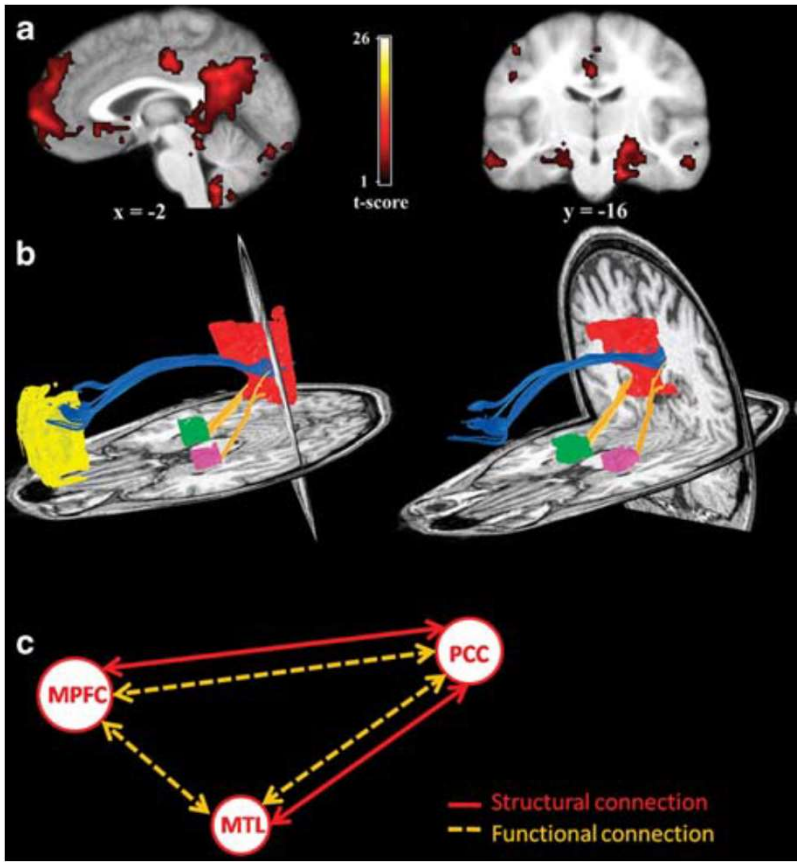

Greicius 2009

Beynin dinlenme durumundaki faaliyetleri

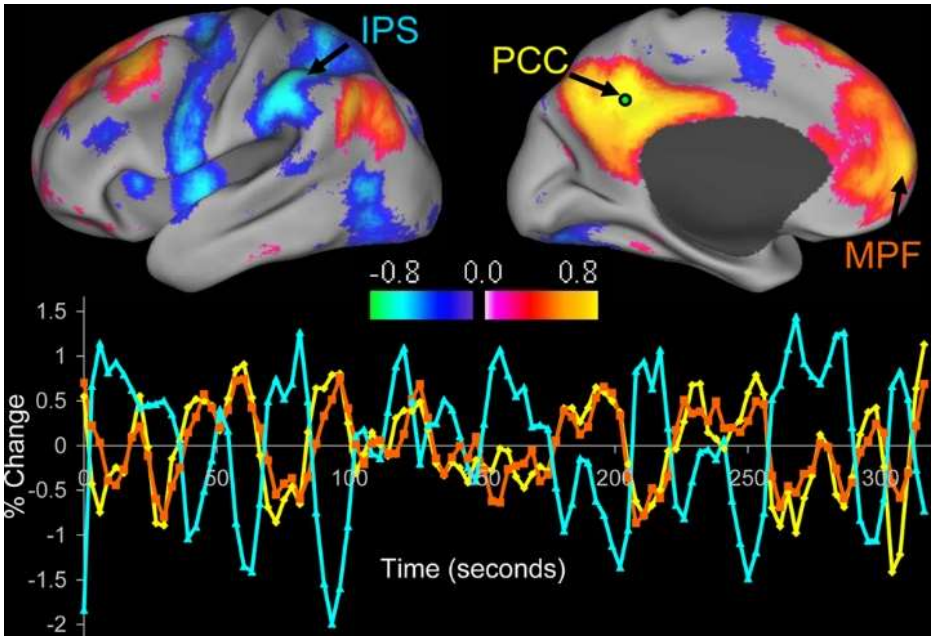

Beynin farklı bilinç düzeylerindeki faaliyetleri

Bitkisel hayat

A diagnosis is only made after repeated examinations that have yielded *no evidence whatsoever* of sustained, reproducible, purposeful, or voluntary behavioral response to visual, auditory, tactile, or noxious stimuli. There must also be no evidence of language comprehension or expression, although there is generally sufficiently preserved hypothalamic and brain-stem autonomic functions to permit survival with medical care. Unlike patients in coma, the vegetative state is characterized by an irregular but cyclic state of circadian sleeping and waking. It is this waking pattern, combined with the wide range of reflexive responses, that are often observed in vegetative patients that can result in this activity being misinterpreted as evidence of volitional (willful) behavior and even the return of conscious awareness.

imagining playing tennis has been shown to elicit activity in the supplementary motor area, a region known to be involved in imagining (as well as actually performing) coordinated movements, in each and every one of 34 participants scanned. In contrast, imagining moving from room to room in a house commonly activates the parahippocampal cortices, the posterior parietal lobe, and the lateral premotor cortices, all regions that have been shown to contribute to imaginary, or real, spatial navigation. In sharp contrast, when healthy volunteers are simply prompted with words such as "tennis" or "house" (with no prior instructions) or even with action sentences containing the same key words such as "The man enjoyed playing tennis" or "The woman looked around her house," no sustained activity is observed in these brain regions[26]

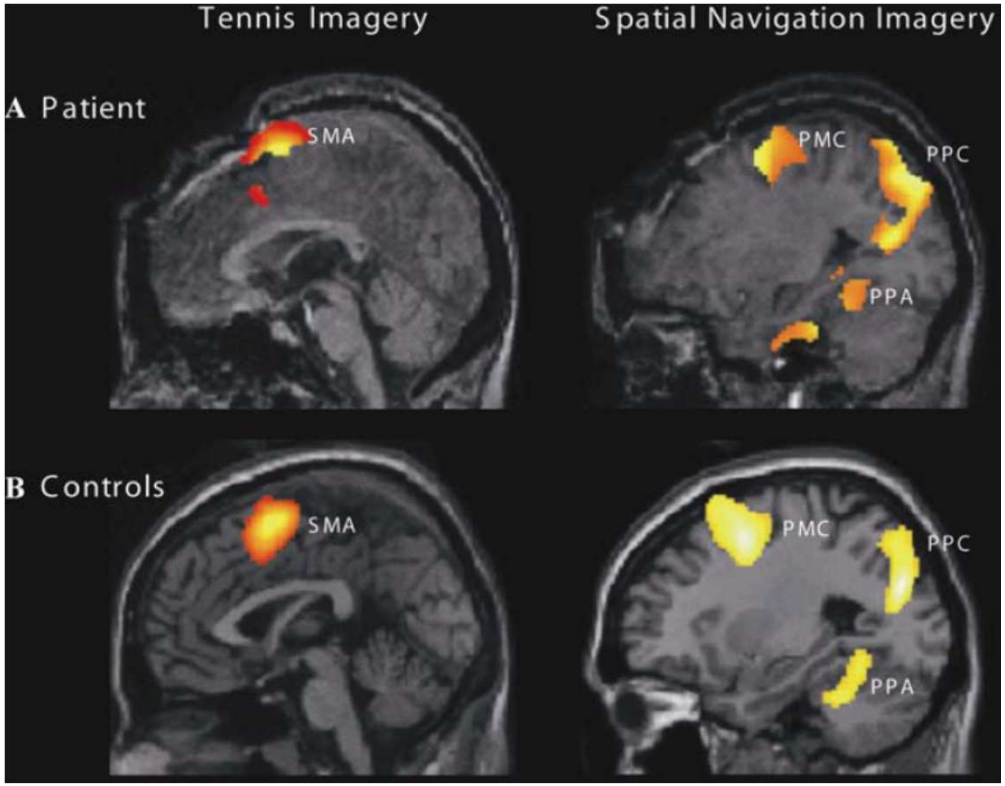

Owen, 2008

Beynin bağlantı haritalaması

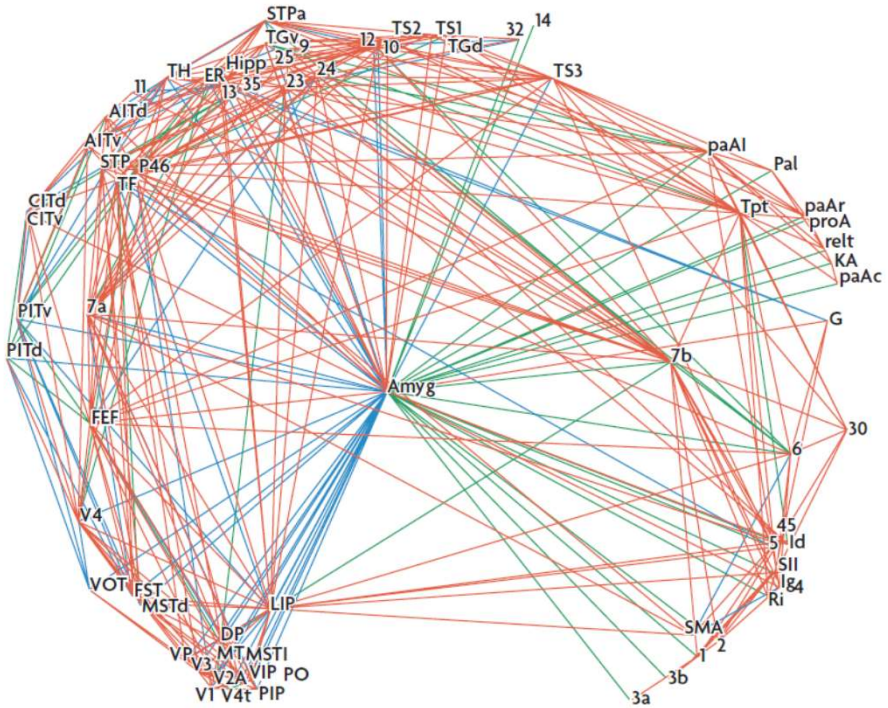

Figure 1 | **Brain connectivity graph.** Quantitative analysis of brain connectivity reveals several clusters of highly interconnected regions (represented by different colours). In this analysis by Young and collaborators[89], the amygdala (Amyg, centre of figure) was connected to all but 8 cortical areas. These connections involved multiple region clusters, suggesting that the amygdala is not only highly connected, but that its connectivity topology might be consistent with that of a connector hub that links multiple provincial hubs, each of which links regions within separate functional clusters. In this manner, the amygdala is hypothesized to be a strong candidate for integrating cognitive and emotional information. Figure labels represent different cortical areas with the exception of Hipp (hippocampus) and Amyg, which represent subcortical areas. Figure reproduced, with permission, from REF. 82 © (1994) Freund Publishing.

Pessoa, 2008

Obje tanımada
çok katmanlı nöron gruplarının görevinin validasyonu

W matrisi

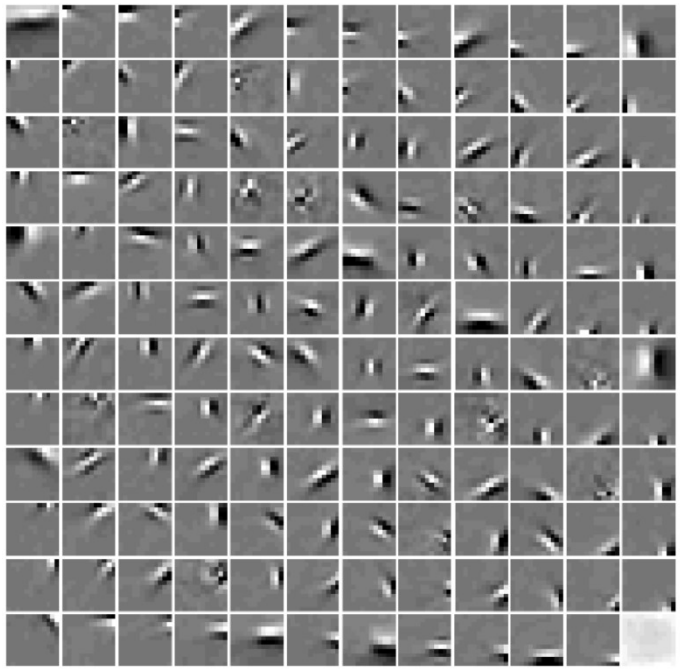

Doğal ortam resimlerinde ICA uygulaması

Lee, Sejnowski, 2000

Multi Layer Perceptron ve Derin Öğrenme

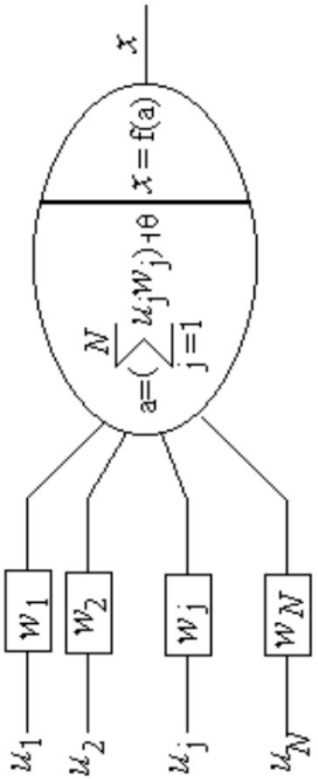

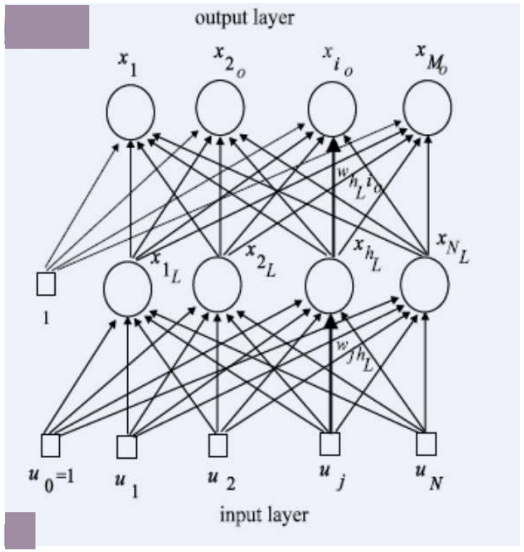

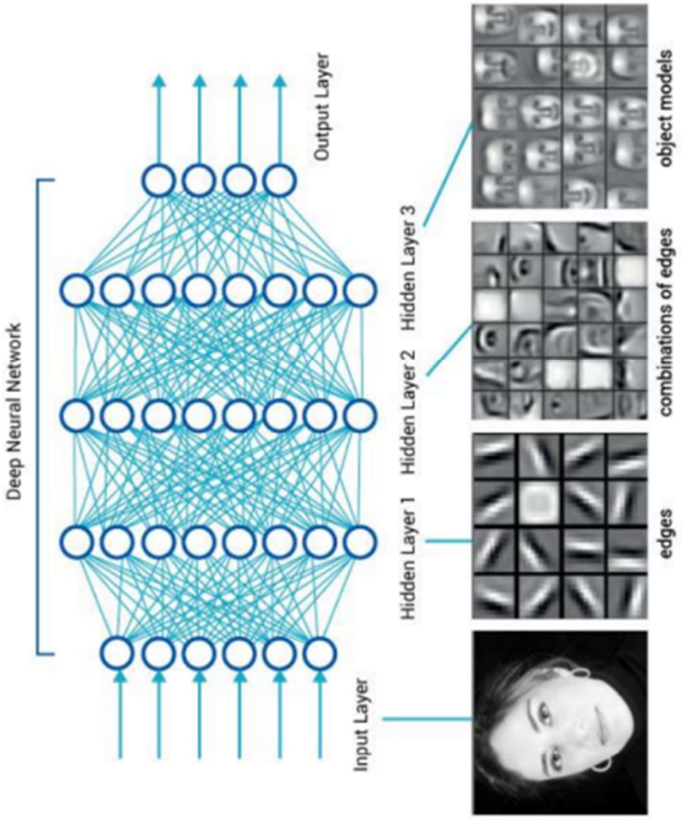

Tekil Elektrod Kayıtları

Invariant visual representation by single neurons in the human brain

R. Quian Quiroga[1,2]†, L. Reddy[1], G. Kreiman[3], C. Koch[1] & I. Fried[2,4]

Vol 435|23 June 2005|doi:10.1038/nature03687

patients had to perform a simple task during all sessions (indicating with a key press whether a human face was present in the image). Performance was close to 100%.

The subjects were eight patients with pharmacologically intractable epilepsy who had been implanted with depth electrodes to localize the focus of seizure onset. For each patient, the placement of the depth electrodes, in combination with micro-wires, was determined exclusively by clinical criteria[13]. We analysed responses of neurons from the hippocampus, amygdala, entorhinal cortex and parahippocampal gyrus to images shown on a laptop computer in 21 recording sessions. Stimuli were different pictures of individuals, animals, objects and landmark buildings presented for 1 s in pseudo-random order, six times each.

We recorded from a total of 993 units (343 single units and 650 multi-units), with an average of 47.3 units per session (16.3 single units and 31.0 multi-units).

The mean number of images in the screening session was 93.9 (range 71–114). The data were quickly analysed offline to determine the stimuli that elicited responses in at least one unit (see definition of response below). Subsequently, in later sessions (testing sessions) between three and eight variants of all the stimuli that had previously elicited a response were shown. If not enough stimuli elicited significant responses in the screening session, we chose those stimuli with the strongest responses. On average, 88.6 (range 70–110) different images showing distinct views of 14 individuals or objects (range 7–23) were used in the testing sessions. Single views of random stimuli (for example, famous and non-famous faces, houses, animals, etc) were also included. The total number of stimuli was determined by the time available with the patient (about 30 min on average).

A response was considered significant if it was larger than the mean plus 5 standard deviations (s.d.) of the baseline and had at least two spikes in the post-stimulus time interval considered (300–1,000 ms). All these responses were highly selective: for the responsive units, an average of only 2.8% of the presented pictures (range: 0.9–22.8%) showed significant activations according to this criterion. This high selectivity was also present in the screening

Tekil Elektrod kaydı

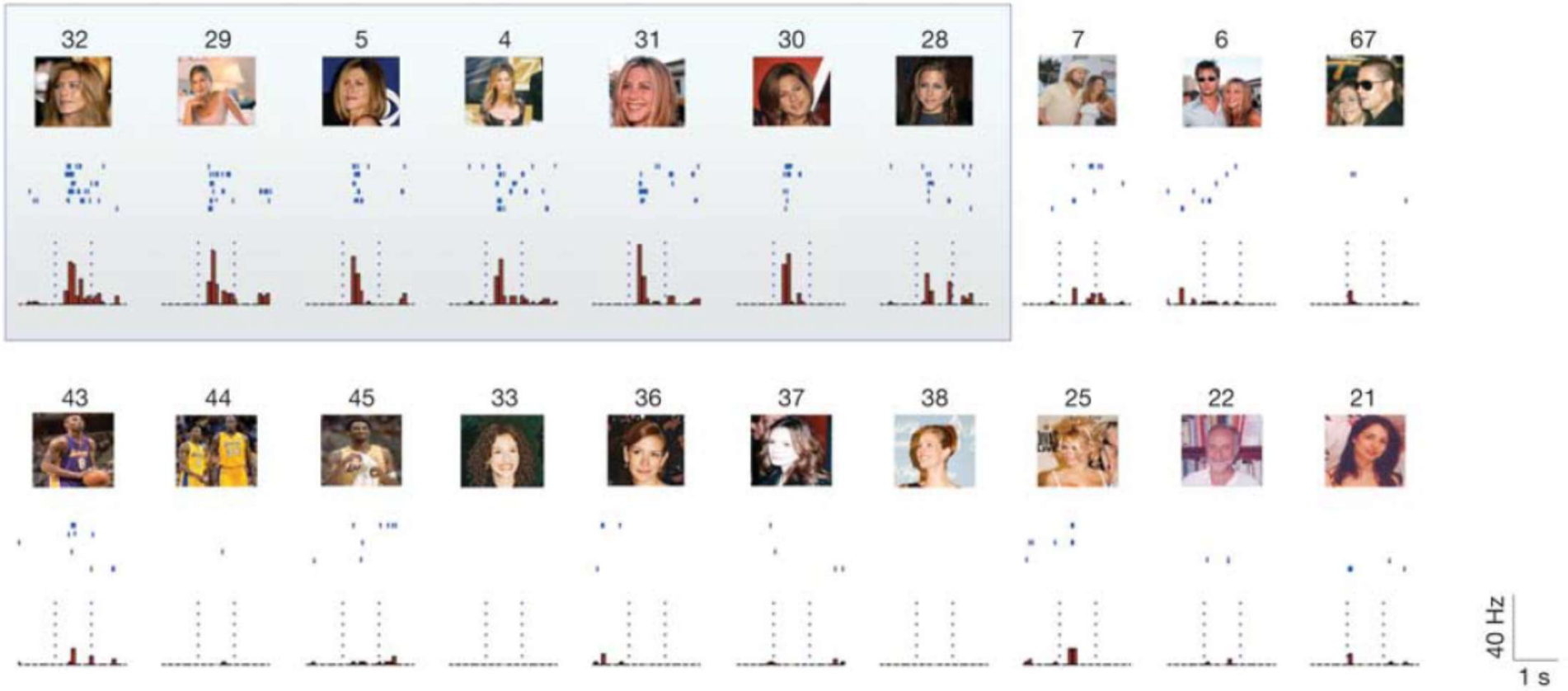

Bir hastaya ait bu elektrod kaydı sadece Jennifer Aniston resimlerine tepki veriyor
(Brad Pitt ile beraberken ise aktif değil!!!)

Tekil Elektrod kaydı

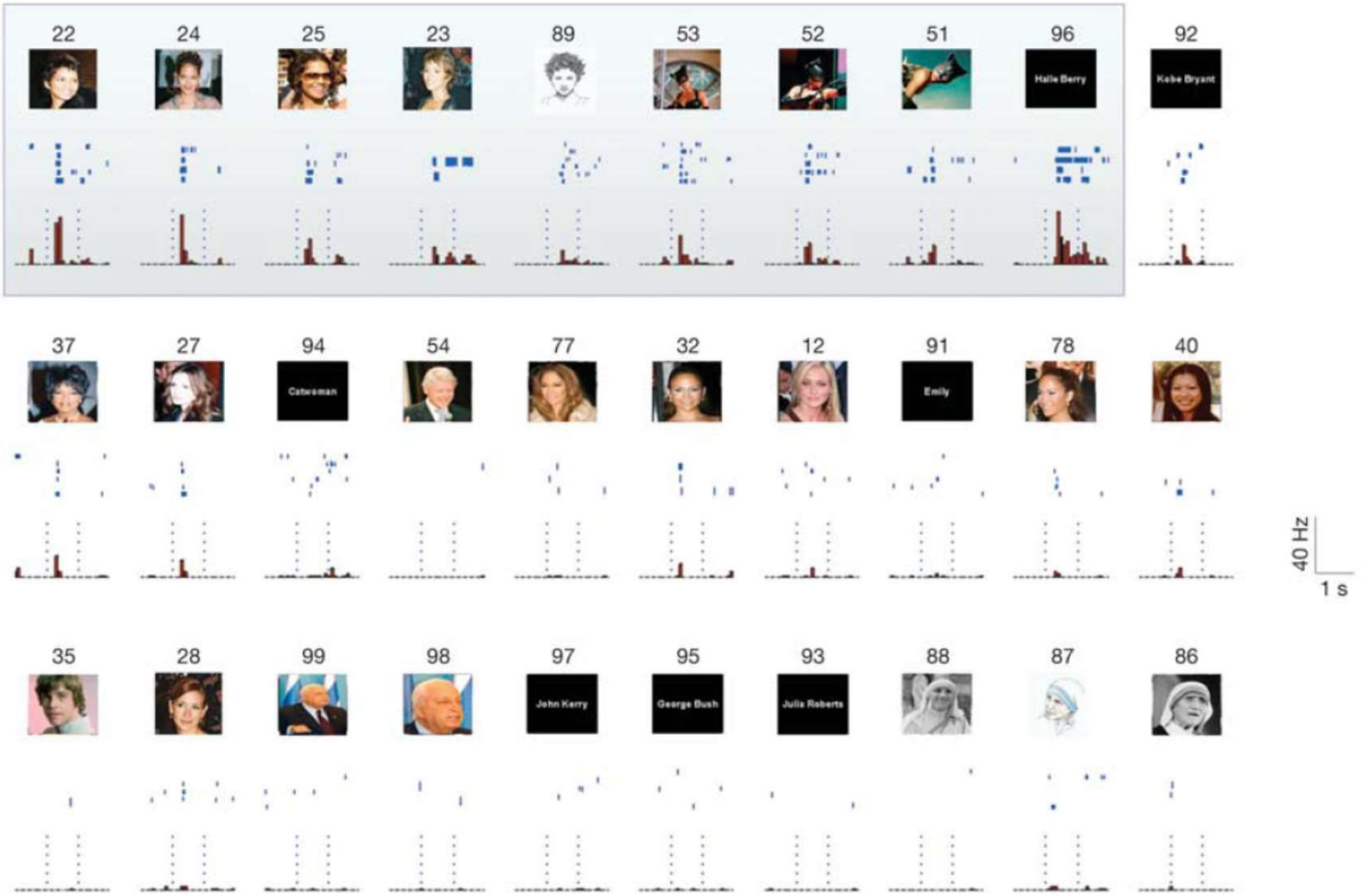

Bir hastanın bir elektrodu sadece Halle Berry resimlerine ve hatta ismine ve hatta onun catwoman kostümüne tepki veriyor

Teknik açmazlar

Çakıştırma işleminin sorunları nedeniyle oluşan hatalar

"Voxel-Based Morphometry" Should Not Be Used with Imperfectly Registered Images

Fred L. Bookstein

NeuroImage **14**, 1454–1462 (2001)

COMMENTS AND CONTROVERSIES

Why Voxel-Based Morphometry Should Be Used

John Ashburner[1] and Karl J. Friston

NeuroImage **14**, 1238–1243 (2001)

Why voxel-based morphometric analysis should be used with great caution when characterizing group differences

Christos Davatzikos*

NeuroImage 23 (2004) 17–20

Yazılım hataları

FreeSurfer is a popular software package to measure cortical thickness and volume of neuroanatomical structures. However, little if any is known about measurement reliability across various data processing conditions. Using a set of 30 anatomical T1-weighted 3T MRI scans, we investigated the effects of data processing variables such as FreeSurfer version (v4.3.1, v4.5.0, and v5.0.0), workstation (Macintosh and Hewlett-Packard), and Macintosh operating system version (OSX 10.5 and OSX 10.6). Significant differences were revealed between FreeSurfer version v5.0.0 and the two earlier versions. These differences were on average 8.8±6.6% (range 1.3–64.0%) (volume) and 2.8±1.3% (1.1–7.7%) (cortical thickness).

The observed differences are similar in magnitude as effect sizes reported in accuracy evaluations and neurodegenerative studies. The main conclusion is that in the context of an ongoing study, users are discouraged to

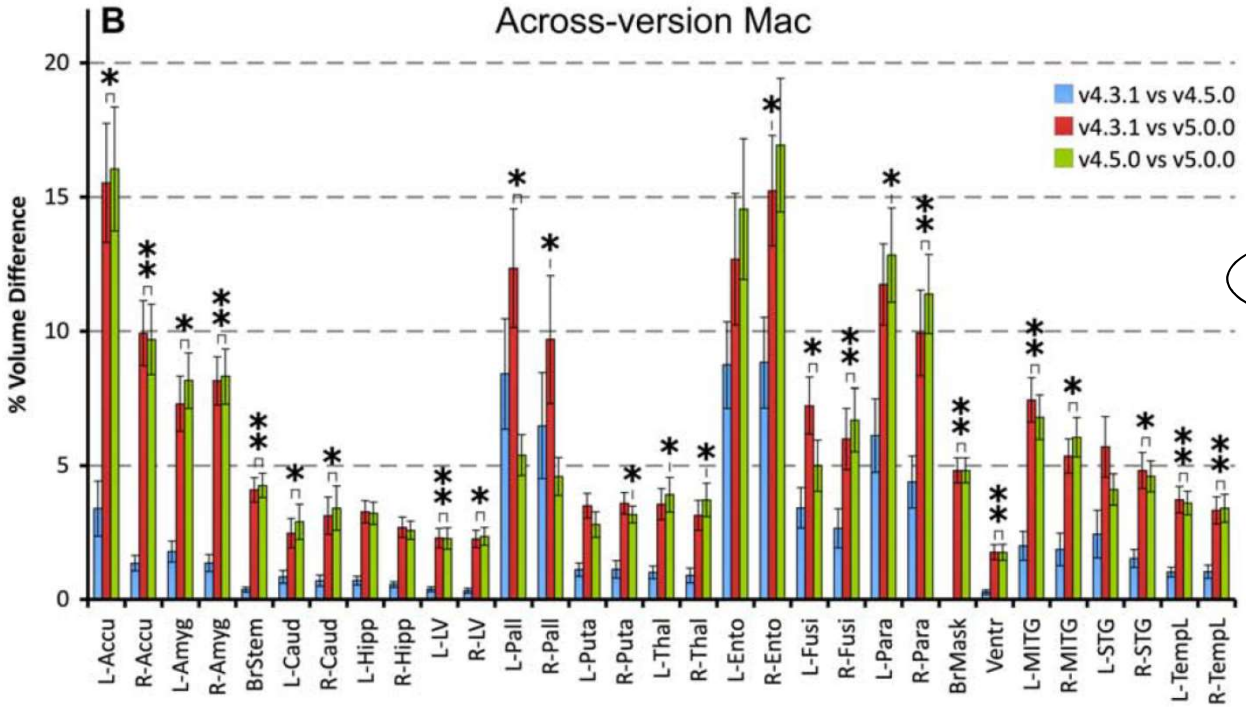

Gronenschild, 2012

Istatistiksel hatalar

Subject. One mature Atlantic Salmon (Salmo salar) participated in the fMRI study.

Task. The task administered to the salmon involved completing an open-ended mentalizing task. The salmon was shown a series of photographs depicting human individuals in social situations with a specified emotional valence. The salmon was asked to determine what emotion the individual in the photo must have been experiencing.

Design. Stimuli were presented in a block design with each photo presented for 10 seconds followed by 12 seconds of rest. A total of 15 photos were displayed. Total scan time was 5.5 minutes.

Preprocessing. Image processing was completed using SPM2. Preprocessing steps for the functional imaging data included a 6-parameter rigid-body affine realignment of the fMRI timeseries, coregistration of the data to a T_1-weighted anatomical image, and 8 mm full-width at half-maximum (FWHM) Gaussian smoothing.

Analysis. Voxelwise statistics on the salmon data were calculated through an ordinary least-squares estimation of the general linear model (GLM). Predictors of the hemodynamic response were modeled by a boxcar function convolved with a canonical hemodynamic response. A temporal high pass filter of 128 seconds was include to account for low frequency drift. No autocorrelation correction was applied.

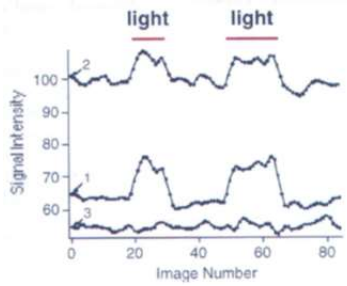

GLM RESULTS

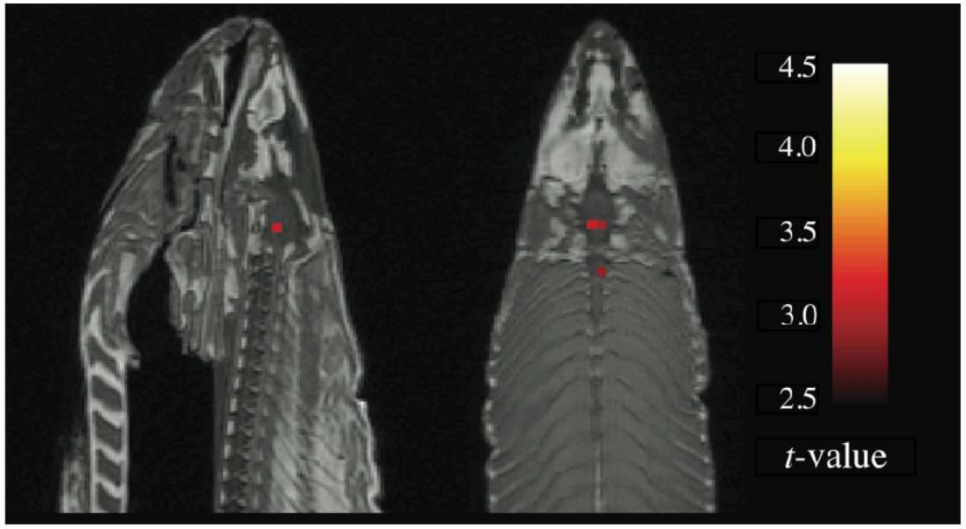

Out of a search volume of 8064 voxels a total of 16 voxels were significant.

Identical *t*-contrasts controlling the false discovery rate (FDR) and familywise error rate (FWER) were completed. These contrasts indicated no active voxels, even at relaxed statistical thresholds ($p = 0.25$).

Bennet et al, 2009

Istatistiksel hatalar

Ayağı x numara ve üstü olanlar erkektir
x=40 ya da 41 ya da 42 ya da 43 ya da 44 ya da 45 ya da 46

1. Tip hata: x numara ayağı olan kadın (false positive)
2. Tip hata: x-1 numara ayağı olan erkek (false negative)

Çareler: Bonferronni (1995), FEW, FDR

Functional MRI (fMRI) is 25 years old, yet surprisingly its most common statistical methods have not been validated using real data. Here, we used resting-state fMRI data from 499 healthy controls to conduct 3 million task group analyses. Using this null data with different experimental designs, we estimate the incidence of significant results. In theory, we should find 5% false positives (for a significance threshold of 5%), but instead we found that the most common software packages for fMRI analysis (SPM, FSL, AFNI) can result in false-positive rates of up to 70%. These results question the validity of some 40,000 fMRI studies and may have a large impact on the interpretation of neuroimaging results.

A total of 2,880,000 random group analyses were performed to compute the empirical false-positive rates of SPM, FSL, and AFNI; these comprise 1,000 one-sided random analyses repeated for 192 parameter combinations, three thresholding approaches, and five tools in the three software packages.

ROI

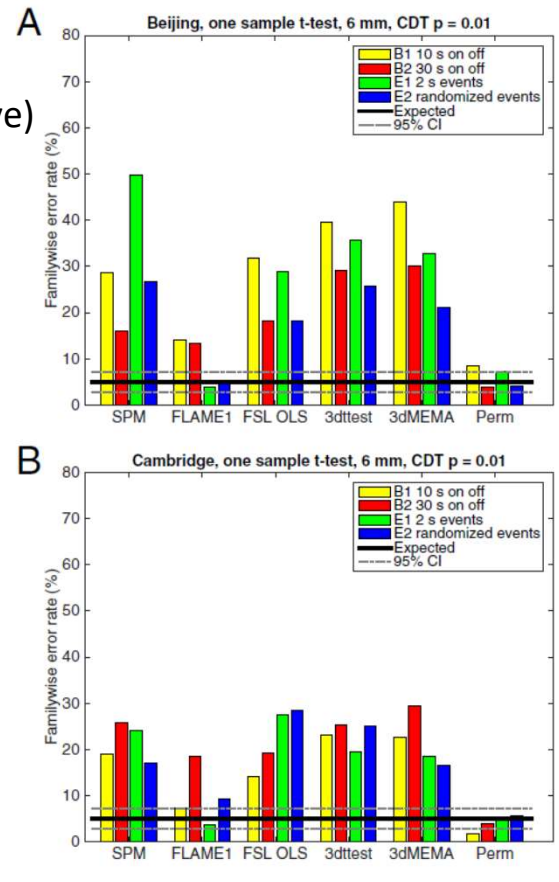

voksel

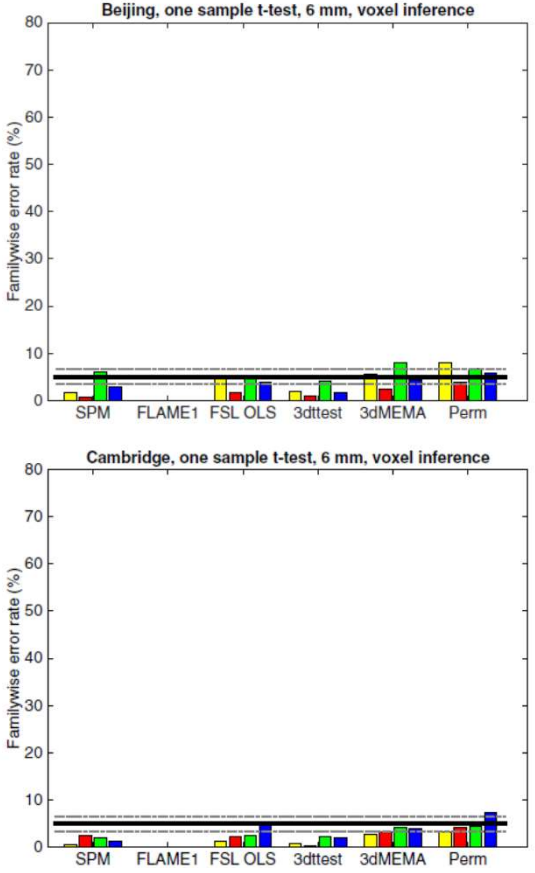

Eklund, 2016

- Özetlenen hataların çoğu yetersiz kalite kontrolünden kaynaklanmaktadır.
- Bu nedenle özellikle 2005 öncesindeki nörogörüntüleme literatüründe pek çok tutarsız sonuç mevcuttur.

Fırsatlar

Veri paylaşımı inisiyatifleri

Temel araştırma fonları:

1. Human Brain Project: Simulasyon ve hesaplama
2. Brain Initiative: Araç geliştirme

Grup Çalışmaları:

Connectome
INCF

Atlas erişimi

Veri bankaları:

NITRC
ADNI
LONI

Makine öğrenmesi uygulamaları

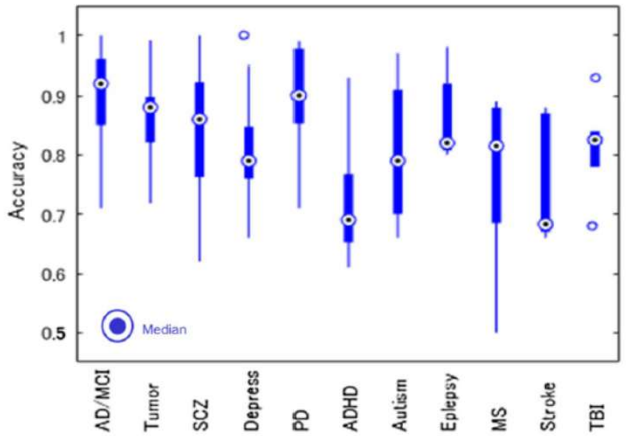

Fig. 5 Disorder-specific box plots of reported overall accuracies of the surveyed papers. Dot including circles indicate the median accuracy

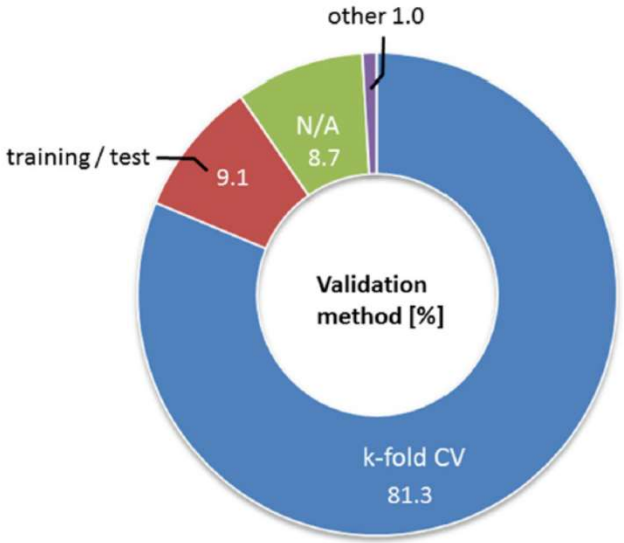

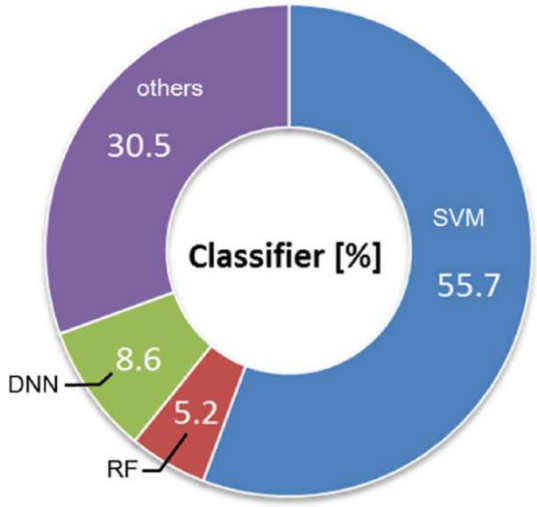

Fig. 6 Classifiers used for ML of the surveyed papers

Sakai, Yamada, 2019

Çok çekirdekli süper bilgisayar uygulamaları

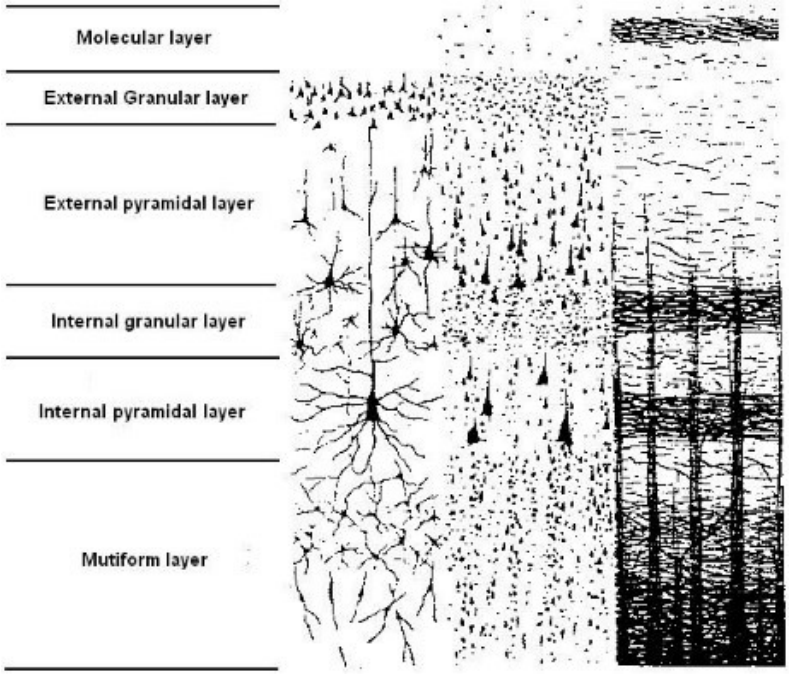

Fig. 1. Blue Brain information storage

Henry Markram, Blue Brain Project

Çok çekirdekli süper bilgisayar uygulamaları

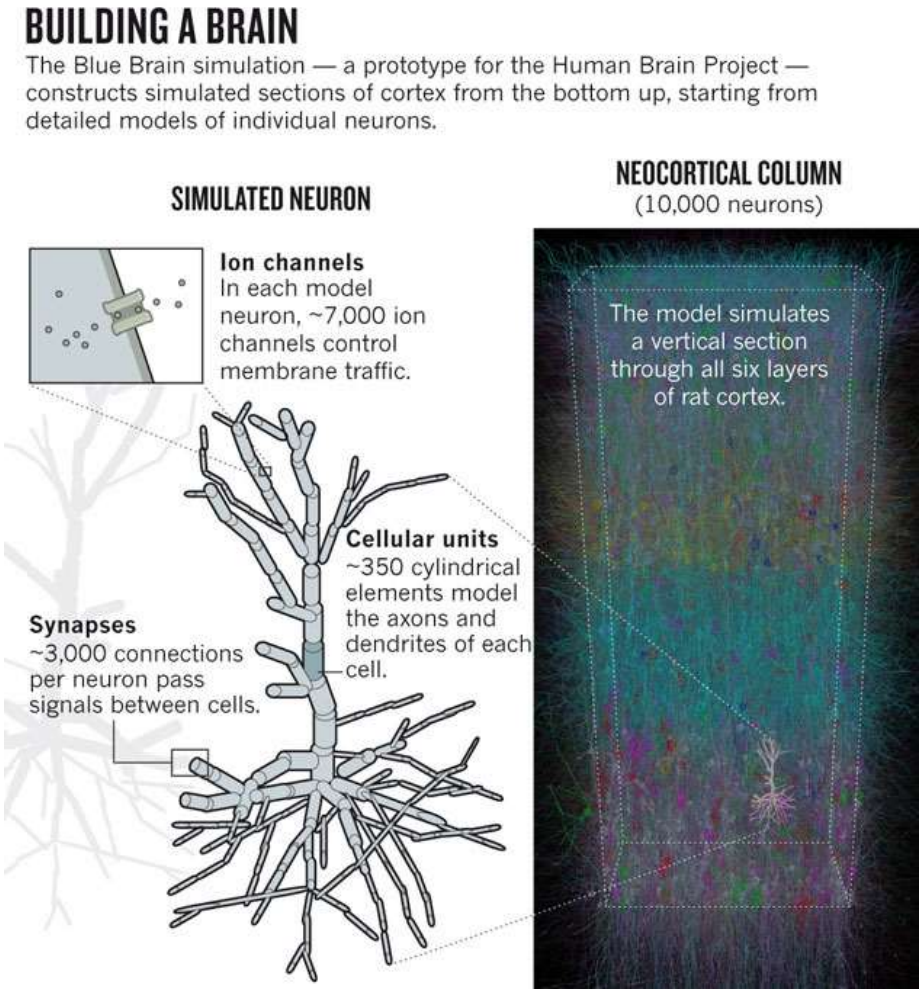

REQUIREMENTS

The hardware & software required to build a Blue Brain…

- 8,096 CPUs at 700 MHz each of which can map one or two simulated brain neurons
- 256MB to 512MB memory per processor.
- 100 kilowatts power consumption.
- Processor with a very high processing power.
- 22.8 TFLOPS peak processing speed.
- Linux and C++ software.

Lishita Shah

Çok çekirdekli süper bilgisayar uygulamaları

Human Brain Project

Extremely Scalable Spiking Neuronal Network Simulation Code: From Laptops to Exascale Computers

Jakob Jordan[1], Tammo Ippen[1,2], Moritz Helias[1,3], Itaru Kitayama[4], Mitsuhisa Sato[4], Jun Igarashi[5], Markus Diesmann[1,3,6] and Susanne Kunkel[7,8]*

Frontiers, Neuroinformatics, 2018

İşlemci bağlantı haritaları ve işlemcilerin bellek kullanımı optimize edilecek şekilde yeniden düzenleniyor

Bitirirken...

Geride bıraktığımız yaklaşımlar

Sansasyonel kategorizasyonlar: Sağcıların amigdalası, solcuların prefrontal korteksi büyük

Haddini aşan kestirimler: Ne düşündüğünü biliyorum

Popüler uygulama girişimleri: Sadakat testi

Pragmatik uygulamalar: Nöromarketing

25 sene sonunda: Mahalle terzisinin yerini konfeksiyon almış, teğelin yerini makine dikişi almış, küçük üretimler gerçek sanatçısına kalmıştır.

Geleceğe yönelik hayallerimiz

Neil Harbisson:
Görsel implant sayesinde renkleri duyabiliyor

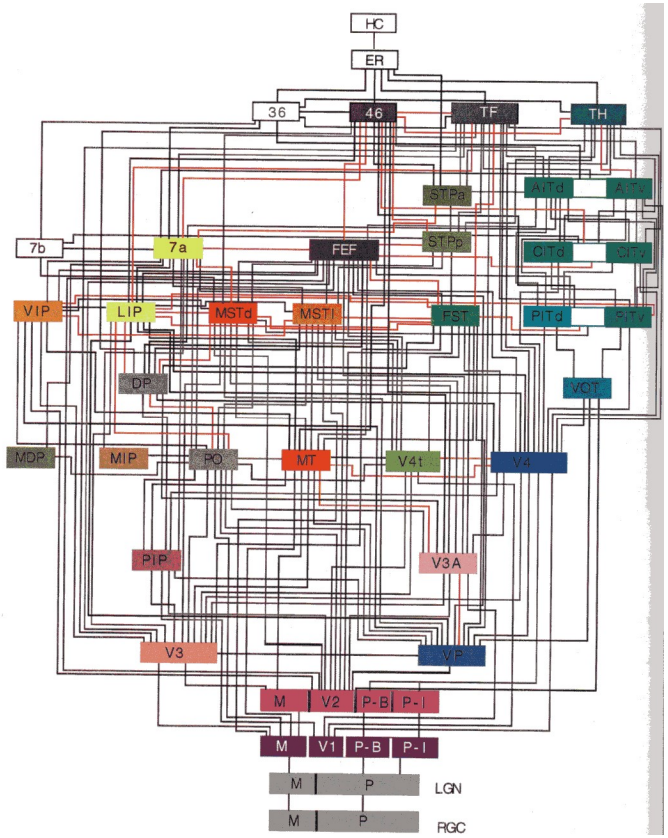

Van Essen, 1991

Gerçekten çok karmaşık olan bu görsel korteks haritası yerine daha da karmaşık yapay bir harita olsa, buna kim itiraz edebilir?

1970’ler: ‘Space.... The final frontier’

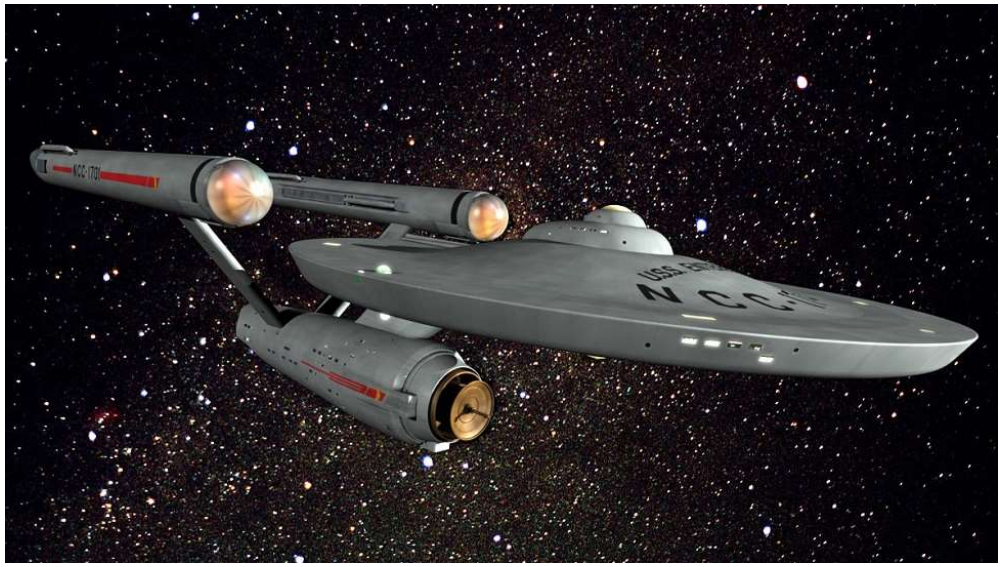

2020’ler: ‘Brain.... The final frontier’

TEŞEKKÜRLER